



# Remote sensing for vegetation monitoring in carbon capture storage regions: A review



Yun Chen<sup>a,\*</sup>, Juan P Guerschman<sup>a</sup>, Zhibo Cheng<sup>b</sup>, Longzhu Guo<sup>c</sup>

<sup>a</sup> CSIRO Land and Water, Canberra, ACT 2601, Australia

<sup>b</sup> Shihezi University, Xinjiang 832003, China

<sup>c</sup> Hohai University, Nanjing 210098, China

## HIGHLIGHTS

- An overview of remote sensing systems and applications in vegetation monitoring.
- A review on detecting CO<sub>2</sub> leakage effect on vegetation using hyperspectral imaging.
- Identification of major issues on distinguishing CO<sub>2</sub> leakage-derived plant stress.
- Recommendation on an integrated remote-sensing monitoring system at CCS sites.

## ARTICLE INFO

### Keywords:

CCS  
CO<sub>2</sub> emission  
Leakage effects  
Vegetation condition  
Stress detection  
Hyperspectral imaging

## ABSTRACT

Carbon Capture and Storage (CCS) is an emerging climate change mitigation technology which prevents carbon dioxide (CO<sub>2</sub>) from entering the atmosphere, so as to reduce greenhouse gas emissions. Environmental monitoring in CCS sites is critical for ensuring that any CO<sub>2</sub> leakage and its effect on biota, especially vegetation, is detectable. It also plays an important role in creating a social license to operate and assuring the general public that the mechanisms for leak detection and remediation are in place. This review overviews current remote sensing technologies for vegetation monitoring of CCS sites/regions (with a focus on rangelands and pastures), including medium-to-high resolution satellite, aerial (both manned and unmanned aircrafts) and *in situ* sensors and methods. Our literature survey has pointed out that remote sensing, particularly hyperspectral sensors, can accurately detect CO<sub>2</sub> leakage derived effects on vegetation. It can compensate the two main drawbacks of operational systems for detecting these effects over large areas. One is the areas affected tend to be relatively small (1–15 m); and the other is symptoms in vegetation tissues tend to be similar to other stresses, such as nutrient or water deficiency. With this in mind, we have recommend that a comprehensive system should be put in place. It integrates continuous monitoring with ad-hoc detection to assess vegetation conditions in a planned CCS site. Site-based phenocams and area-based medium-resolution satellite remote sensing sources can be used to compare any given point in time (e.g. the injection point) with the condition at the same location in the past. Before an injection commences, a baseline assessment should be conducted using the combination of high-resolution aerial hyperspectral imaging and medium-resolution long-term data from Landsat sensors. Further acquisition of high-resolution aerial imagery (ideally hyperspectral) is particularly useful following specific detected CO<sub>2</sub> leaking events. Aiming at bridging the gaps between research, development and implementation of CCS, this review will contribute to environmental and social impacts of sustainable energy policies, including climate change mitigation and environmental pollution reduction.

## 1. Introduction

### 1.1. Carbon capture and storage technology

Global warming is primarily a result of too much carbon dioxide

(CO<sub>2</sub>) in the atmosphere. CO<sub>2</sub> is predicted to increase substantially over the 21st century. Thus decreasing the total CO<sub>2</sub> output may significantly mitigate the effects and severity of future climate change [1]. This places a premium on developing technology solutions to minimize rises in atmospheric CO<sub>2</sub> levels. Carbon Capture and Storage (CCS) has

\* Corresponding author.

E-mail address: [yun.chen@csiro.au](mailto:yun.chen@csiro.au) (Y. Chen).

<https://doi.org/10.1016/j.apenergy.2019.02.027>

Received 29 November 2018; Received in revised form 25 January 2019; Accepted 6 February 2019

Available online 15 February 2019

0306-2619/ © 2019 Elsevier Ltd. All rights reserved.

been endorsed by the Intergovernmental Panel on Climate Change (IPCC) as part of a portfolio of measures to mitigate climate change [2]. Nowadays pilot projects multiply all around the world. An assessment on environmental and social impacts of this energy policy relating to climate change mitigation and environmental pollution reduction has always been essential.

CCS is an emission reduction process that captures up CO<sub>2</sub> emissions produced from the use of fossil fuels in electricity generation and industrial processes, preventing large amounts of CO<sub>2</sub> from being released into the atmosphere [3]. The technology involves three major steps: capture, transport and injection/storage. CO<sub>2</sub> is firstly separated from other gases produced at facilities and compressed to a liquid state. It is usually transported to a suitable site for geological storage using pipelines. CO<sub>2</sub> is then injected into deep, underground rock formations, commonly at depths of one kilometre or more. These porous formations into which CO<sub>2</sub> is injected for permanent storage are often referred to as deep saline formations or saline reservoirs. They are almost always sedimentary rocks such as sandstones or limestones [4].

Although technically feasible with current technology, large-scale adoption of CCS needs to address its safety and effectiveness [5]. Of primary concern is the possibility of CO<sub>2</sub> leaking from storage sites. A significant risk is that a leak may migrate to the Earth's surface and adversely affect water quality, soil properties, flora and fauna [6]. Based on both IPCC [2] and past research [5], risk of leakage from well-selected, designed and managed geological storage sites is low [2,5]. CO<sub>2</sub> could be trapped for millions of years as exemplified by many natural analogues, and well-located storage sites are likely to retain over 99 per cent of the injected CO<sub>2</sub> over hundreds of years [3]. However, even small leaks may increase soil CO<sub>2</sub> concentrations and atmospheric concentrations below plant canopies. The most likely leakage pathways for CO<sub>2</sub> from a storage site are associated with small-scale features, such as natural interruptions and breaches through the confining strata, faults and fractures, and degraded wells. Intermittent emissions may also occur during periods of CO<sub>2</sub> injection. Therefore, long-term environmental monitoring of CCS sites is critical to the confirmation of storage integrity for ensuring that if the CO<sub>2</sub> stored underground is leaked into the soil, the leaking, as well as the potential effects of CO<sub>2</sub> on the biota, can be detected [7]. On the other hand, it is also a highly-required social licence for public assurance regardless of the low risk of CO<sub>2</sub> leaks and the potential effects of such leaks on the environment.

### 1.2. Detection and monitoring of CO<sub>2</sub> leakage

Monitoring of a CCS site can be accomplished by many techniques. These include underground measurements and near-surface detection, each offers unique strengths [8]. The former consists of well pressure monitoring, seismic detection, and predictive modelling of the injected plume in the subsurface; and the latter contains at- or above-surface sampling and remote sensing methods for detecting CO<sub>2</sub> leakage. Among them, near surface detection is a particular key [9]. It is well-known that these traditional ground-based observation methods have the advantages of high precision and reliability [10–13]. However, they are constrained by the distribution and number of observation sites, and the lack of ability of a wide range of real-time monitoring due to their time-consuming and cost-inefficient characteristics. Recent research into environmental impacts has naturally involved the use and development of new monitoring tools and has posed questions about how to identify CO<sub>2</sub> leakage impacts, which may be spatially small within large areas and over long spans of time. Remote sensing is a promising approach to address these questions [14].

Remote sensing is a cost-effective tool for monitoring land conditions over large areas and on a regular basis. According to the target of a remote sensor, remote sensing technologies and methodologies that are applicable for CCS monitoring can be classified into “direct methods” which directly detect atmospheric concentrations of emitted

CO<sub>2</sub>, and “indirect methods” which means the proxy detection of environmental responses to escaped CO<sub>2</sub> [8]. The indirect remote sensing methods for detection of leaking CO<sub>2</sub> associated with CCS sites are those attempts to look at temperature anomalies, surface deformation and vegetation stress. Vegetation monitoring is of particular relevance to the detection of the potentially significant effects of CO<sub>2</sub> leakage. It is a relatively low-cost means to ensure the social license to operate a CCS site. It is also an explicit way to show to the general public that comprehensive environmental monitoring is in place.

Although increased soil CO<sub>2</sub> levels could have significant effects on vegetation, the impacts of this sort of localised slow-release of CO<sub>2</sub> in soil on plant across a large injection site are not yet well understood [15,16]. In the few manipulative experiments and natural settings where CO<sub>2</sub> is present in the soil at very high concentrations, a deleterious effect on vegetation condition is observed as CO<sub>2</sub> causes anoxia in the roots [17,18]. If the effect is present for a prolonged period, it drives plants into chlorosis and eventually into senescence [19]. Smith [20] found the patches of decreased plant growth in a gas (similar to CO<sub>2</sub>) field were approximately 2 m in diameter and were situated at about 10 m intervals that perhaps coincided with joints in the gas pipeline. This is consistent with observations made by Hoeks [21] who stated that the radius of the sphere of influence of a gas leak could vary from 1 to 15 m depending on the size of the leak, soil type and moisture content. Also, Feitz et al. [22] observed the visible extent of the CO<sub>2</sub> leak impact on the plants was limited to small sections directly horizontal above the well and typically defined by a circular pattern, between 5 and 15 m in diameter.

Sensors mounted on satellites and/or aircraft (either manned or unmanned) could be used for detecting changes in vegetation condition in CCS areas. The increasing availability of remotely sensed images due to the rapid advancement of remote sensing technology has expanded the horizon of our choices of imagery sources. Multi-spatial, multi-spectral and multi-temporal data at multi-scales can be provided to suit different purposes, in particular during the last decade. For example, detection of the effects of CO<sub>2</sub> leakage on vegetation with remote sensing methods can be done accurately, especially when using hyperspectral sensors [23]. Operational systems for the detection of these CO<sub>2</sub>-derived effects on vegetation over large areas have, however, two main drawbacks. One is that the areas affected tend to be relatively small, and the other is that the symptoms in vegetation tissues tend to be similar to the stress caused by other factors, such as nutrient or water deficiency, which creates a high rate of false positives. Vegetation monitoring in this context needs to determine natural vegetation variability both in space and over time. There are many studies and reviews on the topic of vegetation remote sensing in the literature. However, there is an absence of updated critical/comprehensive reviews on research advances related to the rapid development and applications in remote sensors with medium-high spatial/spectral resolutions in vegetation monitoring for CCS projects.

### 1.3. Scope of review

The goal of this review is to offer readers with reference to the use of the most advanced remote sensing technologies/systems to date for addressing major issues and challenges on monitoring the impact of CO<sub>2</sub> leakage on vegetation in CCS sites. Our review is on the existing literature on detecting and monitoring near-surface effects of CO<sub>2</sub> leaks on rangeland and pastures using optical remote sensing techniques, including satellite, aerial (both manned and unmanned aircrafts) and *in situ* methods.

The review is organised as follows: Section 2 presents an overview of remote sensing systems and other technologies which may be suitable for vegetation monitoring in CCS sites, Section 3 describes remote sensing methodologies for detecting vegetation response to CO<sub>2</sub> leakage, with a focus on hyperspectral imaging applications in CO<sub>2</sub> leakage detection, and Section 4 concludes the review by providing

**Table 1**

Main characteristics of commonly used space-borne remote sensors for vegetation detection: spatial resolution, temporal resolution, spectral resolution (bands), spatial coverage (swath), data cost, data availability and scale of application.

Sensor group	Satellite/sensor	Bands	Spatial resolution (m)	Temporal resolution (day)	Max swath at nadir (km)	Scale of application <sup>a</sup>	Data distribution policy (cost)	Data availability
Medium resolution sensor	Landsat	4–9	15–80	16	185	L-G	no	1972–
	SPOT	4–5	2.5–20	26	120	L-R	yes	1986–
	Aster	14	15–90	16	60	L-G	no	1999–
	Sentinel-2	13	10–60	5	290	L-R	no	2015–
High resolution sensor	IKONOS	5	1–4	1.5–3	11.3	L-R	yes	1999–
	QuickBird	5	0.61–2.24	2.7	16.5	L	yes	2001–
	WorldView	4–17	0.31–2.40	1–4	17.6	L	yes	2007–
	RapidEye	5	5	1–5.5	77	L-R	yes	2008–
	Ziyuan III (ZY-3)	4	2.1–5.8	5	50	L-R	yes	2012–
	Gaofen(GF1-4)	5	1–16	4–5	800	L-R	yes	2013–

<sup>a</sup> L = Landscape, R = Regional, G = Global, L-R = Landscape to Regional, L-G = Landscape to Global, R-G = Regional to Global.

recommendations on the development of a broad scale vegetation monitoring system for CO<sub>2</sub> storage areas.

## 2. Remote sensing systems for vegetation monitoring

The medium (10–200 m) to high (< 10 m) resolution satellite sensors which have been widely used for vegetation monitoring are listed in Table 1 for a quick reference. In summary, most optical sensors can be and have been used to detect vegetation changes. There tends to be a trade-off between spatial resolution and temporal frequency. Spatial resolution is an important factor to be considered. Higher spatial resolution sensors are generally able to detect vegetation change with a higher accuracy, but their temporal resolution is usually lower, which hampers intensive temporal monitoring. For extremely high spatial resolution (< 5 m) images, shadow problems, computation issues and data availability are major defects. Therefore, high resolution is not always good for all situations. It is critical to choose remote sensing data with resolution appropriate to the size of the objects that are to be detected.

### 2.1. Satellite medium-high resolution systems

#### 2.1.1. Landsat, Sentinel-2

Landsat is one of the most successful satellite series in history. successively supplying medium resolution (10–200 m) images for over 40 years. The sensors onboard early Landsat missions were Multispectral Scanner (MSS), and later upgraded to Thematic Mapper (TM) on Landsat-4 (launched in 1982), Landsat-5 (launched in 1984) and Enhanced Thematic Mapper Plus (ETM+) on Landsat-7 (launched in 1999). Landsat-5, in particular, has operated for an unexpectedly long period, which makes applications of Landsat TM images in vegetation change detection very common. Launched in 2013, Landsat-8 is the most recent Landsat satellite. The Operational Land Imager (OLI) onboard is the latest optical sensor. The spatial resolutions of these Landsat sensors have been gradually improved from 80 m for MSS to 30 m (15 m for Pan) for TM. Resolutions at this level are ideal for detecting the dynamics of almost all kinds of vegetation (Table 2).

Sentinel-2 is a land monitoring constellation of two identical satellites, Sentinel-2a (launched in 2013) and Sentinel-2b (launched in 2017) by the European Space Agency. The two satellites operate simultaneously, phased at 180° to each other, in a sun-synchronous orbit at a mean altitude of 786 km. The mission provides high resolution optical imagery for the continuity of current Landsat missions. It is designed to make a global coverage of the Earth's land surface every 10 days with one satellite and 5 days with two satellites. The MultiSpectral Instrument (MSI) onboard Sentinel-2 provides high quality multispectral images with spatial resolutions ranging from 10 to 60 m (Table 2).

#### 2.1.2. Worldview and Planet

DigitalGlobe (<https://www.digitalglobe.com>) was founded as WorldView Imaging Corporation in 1992. The company launched its first commercial Earth observation satellite EarlyBird-1 in 1997. The most recent, WorldView-4, was launched in 2016 to become DigitalGlobe's seventh satellite in orbit, joining *Ikonos* which was launched in 1999, QuickBird in 2001, WorldView-1 in 2007, GeoEye-1 in 2008, WorldView-2 in 2009, WorldView-3 in 2014 and WorldView-4 (GeoEye-2) in 2016. It is capable of discerning objects on the Earth's surface as small as 31 cm in the panchromatic and collects multispectral imagery with 1.24 m resolution (Table 3).

Planet (<https://www.planet.com>, formerly known as Planet Labs) is a company based in California that has designed and launched a series of micro-satellites referred to as “Doves” or PlanetScope which make up the world's largest constellation of Earth-imaging satellites. The first two satellites were launched in April 2013. Nowadays with 175+ PlanetScope and 13 SkySat in orbit, Planet is able to image anywhere on Earth daily at 3 m and 72 cm resolution (Table 4). In July 2015 Planet purchased the Blackbridge Geospatial companies which owns a suite of 5 RapidEye satellites together with an extensive network of customers. This gave Planet the capability of accessing the archives of RapidEye imagery (5 m resolution, from 2009) for their commercial applications (Table 4).

Another main source of high-resolution sensors is the Chinese Earth observation system, such as Ziyuan III (or ZY-3) and Gaofen (GF) satellites. The ZY-3-01 satellite was launched in January 2012, and ZY-3-02 reached orbit in May 2016. Together, the two satellites have a revisit-cycle around three days. They are used to provide imagery to monitor resources, land use and ecology, and for use in urban planning and disaster management. GF-1 is the first of a series of seven high-resolution optical Earth observation satellites of China National Space Administration launched on April 2013. It is an analogue to Europe's Copernicus program of Sentinel Earth observation satellites. Another six launches are planned by 2020 and GF 2, GF 3, and GF 4 have already been placed in orbit by March 2018. Gaofen series integrates medium-high spatial resolution imaging capability and a wide swath. These satellites collect different types of environmental data, including all-weather radar imagery and atmospheric measurements. They provide near-real-time observations for disaster prevention and relief, climate change monitoring, geographical mapping, environment and resource surveying, as well as for precision agriculture support. However, there are difficulties in accessing the data from outside China.

#### 2.1.3. Operational systems using medium-high resolution satellites

Remote sensing provides important monitoring datasets at global scale to local scales. The number and range of available datasets have increased rapidly over the last four decades. Correspondingly, these data, in particular Landsat and Sentinel-2, are now widely used in

**Table 2**

Comparisons between Landsat and Sentinel-2 sensors on spatial resolution, temporal resolution, spectral resolution (bands) and spatial coverage (swath).

	Landsat 4 and 5 Thematic Mapper (TM)	Landsat 7 Enhanced Thematic Mapper Plus (ETM +)	Landsat 8 Enhanced Thematic Mapper Plus (ETM +)	Sentinel-2A and Sentinel-2B
Spectral Resolution (nm)	1. 450–520 (B) 2. 520–600 (G) 3. 630–690(R) 4. 760–900 (NIR) 5. 1550–1750 (MIR) 6. 2080–2350 (MIR) 7. 10400–12500 (TIR)	1. 450–520 (B) 2. 520–600 (G) 3. 630–690(R) 4. 760–900 (NIR) 5. 1550–1750 (MIR) 6. 2080–2350 (MIR) 7. 10400–12500 (TIR) 8. 520–900 (Pan)	1. 430–450 (C/A) 2. 450–520 (B) 3. 530–600 (G) 4. 630–680 (R) 5. 850–890 (NIR) 6. 1560–1660 (SIR) 7. 2100–2300 (SIR) 8. 500–680 (Pan) 9. 1360–1390 (C) 10. 10300–11300 (LIR) 11. 11500–12500(LIR)	1. 430–450 (C/A) 2. 460–520 (B) 3. 540–580 (G) 4. 650–680 (R) 5. 700–710 (VRE) 6. 730–750 (VRE) 7. 770–790 (VRE) 8. 780–900 (NIR) 8A. 860–880 (NNIR) 9. 940–960 (WV) 10. 1370–1390 (C) 11. 1570–1660 (SIR) 12. 2100–2280 (SIR)
Spatial Resolution (m)	30 × 30 120 × 120 (TIR)	15 × 15 (Pan) 30 × 30 60 × 60 (TIR)	15 × 15 (Pan) 30 × 30 100 × 100 (TIR)	10 × 10 (Pan) 20 × 20 60 × 60 (TIR)
Temporal Resolution (revisit days)	16	16	16	5
Spatial coverage (km)	185 × 185	183 × 170	185 × 185	290 × 290
Website	<a href="https://lta.cr.usgs.gov/TM">https://lta.cr.usgs.gov/TM</a>	<a href="https://landsat.gsfc.nasa.gov/the-enhanced-thematic-mapper-plus/">https://landsat.gsfc.nasa.gov/the-enhanced-thematic-mapper-plus/</a>	<a href="https://landsat.gsfc.nasa.gov/landsat-8/">https://landsat.gsfc.nasa.gov/landsat-8/</a>	<a href="https://sentinel.esa.int/web/sentinel/missions/sentinel-2">https://sentinel.esa.int/web/sentinel/missions/sentinel-2</a>

Note: B = blue, G = green, R = red, C/A = coastal/aerosol, NIR = near-infrared, NNIR = narrow-band near-infrared, SIR = short-wavelength infrared, MIR = mid-wavelength infrared, LIR = long-wavelength infrared, TIR = total infrared, Pan = Panchromatic, C = Cirrus, VRE = Vegetation Red Edge, WV = water vapour.

operational systems to inform management and demonstrate stewardship to meet the demand for property scale data in accessible formats.

One such example in the United States is the online platform developed by Planet (<https://www.planet.com/products/platform>). With the rapid expansion of the imaging capability offered by micro-satellites, the whole business model of Planet is rapidly changing from selling single images to a subscription-based model. The Planet Platform is a fully-automated, cloud-based platform for online image downloading, processing and management. It delivers analysis-ready data enabling customers to build tools, integrate data, run analytics, and extract information at scale. Planet is also approaching governments offering whole-of-government licences to access and use such tools.

An Australian example is the VegMachine® tool (<https://vegmachine.net/>) which has played a pioneering role in delivering remotely sensed land cover data for land management in Queensland (QLD), Australia [23,24]. VegMachine is an online tool that uses satellite imagery to summarise decades of change in Australia's grazing lands. The software uses satellite data to track changes in landscape cover over time and identify the best places to manage grazing pressure through pinpointing areas that require more specific management. At present, VegMachine® offers information on vegetation cover derived from the Landsat satellites series (starting in 1990) and from the Sentinel 2 satellites from 2016. The web tool is open to public use, providing the full level of service for all of Queensland and a subset of services to a large part of Australia. A most recent study by Guerschman et al. [25] has used the VegMachine to access and interrogate the Landsat fractional cover data for analysing the temporal dynamics of vegetation cover (Fig. 1) at a CCS site.

## 2.2. Airborne hyperspectral imaging

Hyperspectral remote sensing is also known as hyperspectral imaging. It started in the early 70s and has been blooming in many application fields since then. The system collects and processes information simultaneously in dozens or hundreds of narrow, adjacent spectral bands from across the electromagnetic spectrum. These measurements make it possible to derive a continuous spectrum for each image cell (pixel) of a scene. A variety of techniques have been developed for data collection. A common format is a push-broom imaging sensor which

performs four sampling operations involved in the collection of spectral image data: spatial, spectral, radiometric, and temporal [26]. Fig. 2 from Shaw and Burke [27] illustrates the resultant three-dimensional hyperspectral data cube. After adjustments for sensor, atmospheric, and terrain effects are applied, these image spectra can be compared with field or laboratory reflectance spectra with the purpose of recognising objects, identifying materials, or detecting processes. In the case of vegetation, hyperspectral imagery gives detailed information on the specific pigments present and their concentration which is highly useful for accurately detecting specific effects caused by nutrient, water and other stress factors. Therefore, hyperspectral imaging has been used since last decade as a suitable tool for studying vegetation response to CO<sub>2</sub> leakage (see Section 3.2 for details). Commonly used hyperspectral sensors are listed in Table 5.

The primary advantage of hyperspectral imaging is its spectral resolution. An entire spectrum acquired at each point allows all available information from the dataset to be mined almost without the needs of prior knowledge and post-processing. Hyperspectral imaging can also take advantage of the spatial relationships among the different spectra in a neighbourhood, enabling more elaborate spectral-spatial models for a more accurate segmentation and classification of the image [28,29]. The main disadvantage is cost. Fast computers, sensitive detectors, and large data storage capacities are needed for analysing hyperspectral data. All of these factors greatly increase the cost of acquiring and processing hyperspectral data.

## 2.3. Unmanned Aerial Vehicle (UAVs)

An Unmanned Aerial Vehicle (UAV), also commonly known as a “drone”, is an aircraft flown from a remote location without a human pilot on board. The term “Unmanned Aircraft System” (UAS) has the same meaning and is currently gaining more international acceptance and the term may replace UAV in the near future. UAVs are, as with miniaturised satellites, a rapidly evolving technology for Earth observation. UAVs can be fitted with instruments to measure surface condition and are often cheaper than flying a piloted aircraft. Previously the main use of UAVs was as an enhancement to the more traditional field sampling devices used in experimental studies (e.g. spectroradiometers, thermal cameras) and operated in the context of sampling. Nowadays UAVs have become an alternative to airborne or

**Table 3**  
Summary specifications of high-resolution satellites launched by DigitalGlobe: spatial resolution, temporal resolution, spectral resolution, operational altitude, data cost, data availability and mission life.

	Ikonos	Quickbird	GeoEye-1	Worldview-1	Worldview-2	Worldview-3	Worldview-4
Spectral Resolution (nm)	445–900 (P) 445–516 (B) 506–595 (G) 632–698 (R) 757–853 (N)	450–900 (P) 450–520 (B) 520–600 (G) 630–690 (R) 760–900 (N)	450–800 (P) 450–510 (B) 510–580 (G) 655–690 (R) 780–920 (N)	400–900 (P)	400–450 (C1) 585–625 (Y) 705–745 (RE) 860–1040 (N)	450–800 (P) 400–1040 (R, RE, C1, B, G, Y, N) 405–2245 (DC, A, G, water, S, C2, Sn) 1195–2365 (S)	450–800 (P) 450–510 (B) 510–580 (G) 655–690 (R) 780–920 (N)
Spatial Resolution (m)	1.83 × 1.57	2.9 × 2.62	1.84 × 0.46	3.6 × 2.5	4.3 × 2.5	5.7 × 2.5	5.3 × 2.5
Panchromatic resolution (m)	0.82	0.65	0.46	0.50	0.46	0.31	0.31
Multispectral resolution (m)	4	2.44/1.63	1.64	N/A	1.85	1.24	1.24
Accuracy specification (m)	9/15	23	3	6.5	6.5	3.5	4
Temporal Resolution (revisit days)	3	1–3	2.1 (0.59 m GSD) 2.8 (0.50 m GSD) 8.3 (0.42 m GSD)	1.7 (1 m GSD) < 5.9 (0.55 m GSD)	1.1 (1 m GSD) < 3.7 (0.52 m GSD)	< 1.0 (1 m GSD) < 4.5 (0.31 m GSD)	< 1.0 (1 m GSD) > 4.5 (Total constellation)
Swath width (km)	11.3	16.8/18	15.3	17.7	16.4	13.2	13.1
Spatial coverage (km)	50 × 112 (M) 11 × 120 (S)	16.8 × 16.8/11.2 × 11.2 (M) 16.8/11.2 × 360 (S)	50 × 300 (M) 28 × 224 (S)	60 × 110 (M) 30 × 110 (S)	96 × 110 (M) 48 × 110 (S)	66.5 × 112 (M) 26.6 × 12 (S)	66.5 × 112 (M) 26.6 × 112 (S)
Operational Altitude (km)	681	450/482	681	496	770	617	617
Data availability	Sep 1999–Jan 2015	Oct 2001–Jan 2015	Sep 2008–7–15	Oct 2007–Jan 2015	Oct 2009–7.25	Sep 2014–10–12	Dec 2016–10–12
Mission life (years)	16	14	yes	> 11	yes	yes	yes
Data distribution policy (costs)	no	yes	yes	yes	yes	yes	yes
Website	<a href="https://www.satimagingcorp.com/satellite-sensors/ikonos/">https://www.satimagingcorp.com/satellite-sensors/ikonos/</a>	<a href="https://www.satimagingcorp.com/satellite-sensors/quickbird/">https://www.satimagingcorp.com/satellite-sensors/quickbird/</a>	<a href="https://www.satimagingcorp.com/satellite-sensors/geoeye-1/">https://www.satimagingcorp.com/satellite-sensors/geoeye-1/</a>	<a href="https://www.satimagingcorp.com/satellite-sensors/worldview-1/">https://www.satimagingcorp.com/satellite-sensors/worldview-1/</a>	<a href="https://www.satimagingcorp.com/satellite-sensors/worldview-2/">https://www.satimagingcorp.com/satellite-sensors/worldview-2/</a>	<a href="https://www.satimagingcorp.com/satellite-sensors/worldview-3/">https://www.satimagingcorp.com/satellite-sensors/worldview-3/</a>	<a href="https://directory.eoportal.org/web/eoportal/satellite-missions/v-w-x-y-z/worldview-4">https://directory.eoportal.org/web/eoportal/satellite-missions/v-w-x-y-z/worldview-4</a>

Note: (1) P = panchromatic, C1 = coastal, A = aerosol, Y = yellow, B = blue, R = red, G = green, RE = red edge, N = near-infrared, S = short-wavelength infrared, C2 = cirrus, DC = desert clouds, W = water, Sn = snow. (2) GSD = Max Pan Ground sample distance, M = Monaural, St = Stereo.

**Table 4**  
Summary specifications of high-resolution satellites launched by Planet (PlanetScope, RapidEye and SkySat) and China (Ziyuan and Gaofen).

	PlanetScope (Dove)	RapidEye	SkySat	Ziyuan III-01 (ZY-3)	Gaofen 1-7 (GF 1-7)
Spectral resolution (nm)	455–515 (B) 500–590 (G) 590–670 (R) 780–860 (N)	440–510 (B) 520–590 (G) 630–685 (R) 690–730 (RE) 760–850 (N)	450–900 (P) 450–515 (B) 515–595 (G) 605–695 (R) 740–900 (N)	500–800 (P) 450–520 (B) 520–590 (G) 630–690 (R) 770–890 (N)	450–900 (P) 450–520 (B) 520–590 (G) 630–690 (R) 770–890 (N)
Spatial resolution (m)	3.0	5	1	5	4–5
Panchromatic resolution (m)	3	5	0.8	2.1	2
Multispectral resolution (m)	3	5	1.0	3.5	8
Accuracy specification (m)	3.0	6.5	30	25	16
Temporal resolution (revisit days)	1	5.5	4–5	5	4
Swath width (km)	77	77	2–8	51	69
Operational altitude (km)	420–475	630	450	506	644.5
Data availability	Jan 2014–	Aug 2008–	Nov 2013–	Jan 2012–	Sep 2013–
Mission life (years)	1–3	7	> 6	5	5–8
Data distribution policy (costs)	yes	yes	yes	yes	yes
Website	<a href="https://www.planet.com/products/planet-imagery/">https://www.planet.com/products/planet-imagery/</a>	<a href="https://www.satimagingcorp.com/satellite-sensors/other-satellite-sensors/rapideye/">https://www.satimagingcorp.com/satellite-sensors/other-satellite-sensors/rapideye/</a>	<a href="https://www.satimagingcorp.com/satellite-sensors/skysat-1/">https://www.satimagingcorp.com/satellite-sensors/skysat-1/</a>	<a href="https://directory.eoportal.org/web/eoportal/satellite-missions/v-w-x-y-z/zy-3a">https://directory.eoportal.org/web/eoportal/satellite-missions/v-w-x-y-z/zy-3a</a>	<a href="https://directory.eoportal.org/web/eoportal/satellite-missions/g/gaofen-1">https://directory.eoportal.org/web/eoportal/satellite-missions/g/gaofen-1</a>

Note: P = panchromatic, B = blue, R = red, G = green, RE = red edge, N = near-infrared.

space platforms for regional mapping.

In terms of the platforms available, and similarly to manned aircraft, the most widespread types of UAVs are planes and helicopters. Planes have the advantage of more stable flight characteristics and higher payloads. Helicopters, on the other hand, can be launched and retrieved more easily than planes. In UAVs, the single propeller of traditional helicopter technology coexists with multiple propeller units known as multicopters (typically with four, six or eight propellers) which provides additional stability and easier control (Fig. 3). The sensors that can be mounted on UAVs are constrained by the payload capacity of the platform. For vegetation monitoring the most common sensors used include red-NIR radiometers (which allows vegetation indices to be calculated), and thermal sensors. LIDAR sensors are also available for UAVs, although such sensors tend to be heavier and need bigger platforms. The eBee Ag UAV from the SenseFly company (<http://www.sensefly.com/drones/ebee-ag.html>) is perhaps the most successful off-the-shelf UAV available to date.

One of the biggest advantages of UAVs is their relatively low price and ease of use. This permits flying over a defined area and collection of data without the limitations of the more traditional aircraft. Repeated measurements on the same day and/or during a certain period are feasible at much lower costs than manned aircrafts. Miniaturisation is the biggest advantage of UAVs, but comes with the greatest disadvantage of limited payload and endurance. Small, cheap UAVs can only carry light instruments and fly short distances.

A large number of companies are already offering image collection services for vegetation monitoring purposes in the developed world and also in developing countries such as South America and Asia. Typically, the services include visible, near-infrared and sometimes thermal imagery [30]. These wavelengths allow vegetation indices and canopy temperature to be estimated and these are used to estimate canopy cover and water stress. Many universities and research institutes are also actively involved in improving the techniques, both the hardware and instrumentation (i.e. designing UAVs which can fly for longer, with more stability and more autonomy) and in designing better techniques and tools for processing and using the data collected.

#### 2.4. Phenocams (in situ)

Monitoring the impacts of environmental change requires an exponential increase in the quantity, diversity, and resolution of field-collected data. Until recently, ground-based collection of time-series image data over long periods was expensive and technically challenging, but advancements in imaging and communication technologies are enabling continuous, widespread monitoring of the environment. Automated digital time-lapse cameras – “phenocams” – can monitor vegetation status and environmental changes over long periods of time [31].

As high-quality, low-cost digital cameras have become more widely available, interest in applying these tools to ecological and environmental studies has expanded. “Near-surface remote sensing” utilizes data from automated ground-based sensors to augment conventional remote-sensing data, and to help bridge the gap between satellite monitoring and traditional on-the-ground observations. “Phenocams” – digital cameras configured to capture time-lapses (or repeat photography) – can provide a permanent, continuous visual record of the environment over years or even decades. Information captured by phenocams can provide essential baseline data for tracking such changes. Phenocam-derived data can also be combined with data obtained from other remote sensors to characterize the relationship between environmental drivers and vegetation responses, as well as for cross-scale comparison and monitoring.

The technologies include: conventional RGB cameras, multispectral and hyperspectral sensors, long-wave infrared and thermal and LIDAR [32]. An example of thermal cameras used for individual wheat plants and for experimental wheat plots is shown in Fig. 4. The main

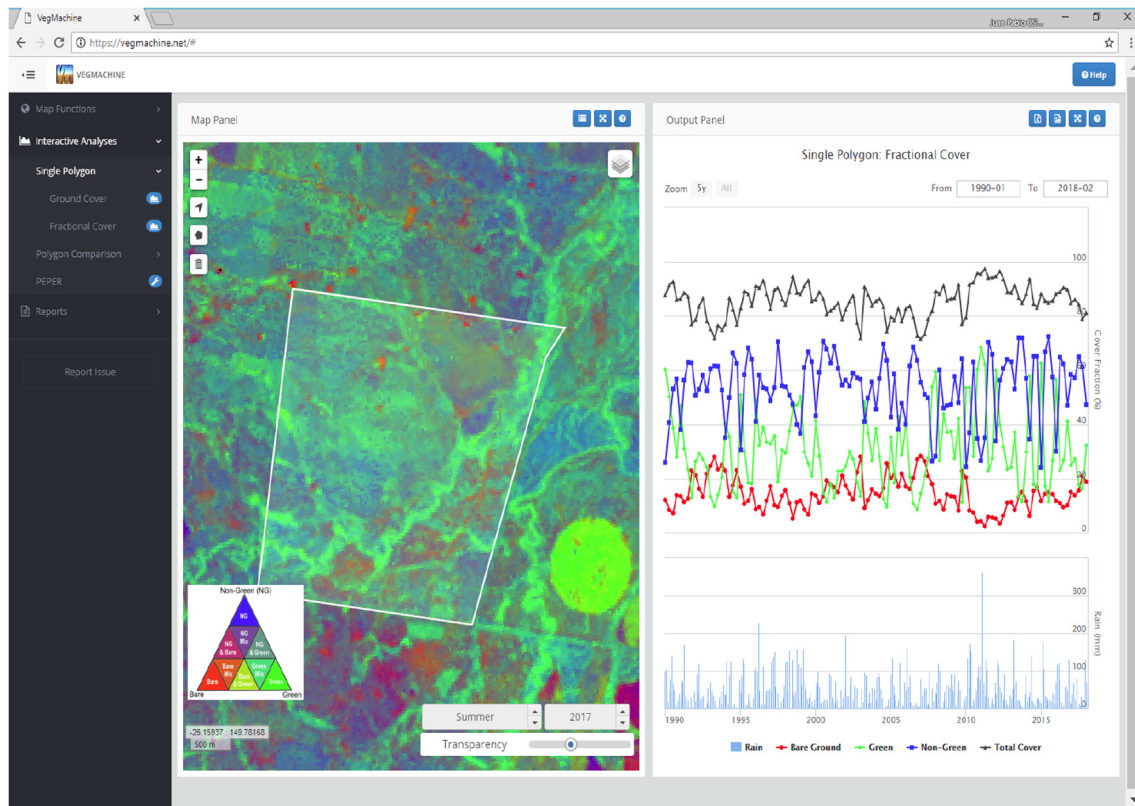


**Fig. 1.** Screen capture of VegMachine® tool showing the fractional cover image for summer 2017 (Dec 2017 to Feb 2018), and the median values for (from top to bottom of the right panel) total cover, non-green vegetation, green vegetation, bare ground and rainfall for the CCS site (left panel) from 1988 to 2017. (For interpretation of the references to color in this figure legend, the reader is referred to the web version of this article.)

difference is that such measurements are made at a much closer distance to the plants, can be near-continuous (many times per day) and additionally, they can be done from varying viewing angles. Therefore, high temporal and spatial resolution imagery from phenocams can be used to obtain information about vegetation changes across a wide range of vegetation types. The field is developing rapidly and continued technological advances are likely to provide further opportunities for image-based, real-time environmental monitoring.

## 2.5. Discussion

Satellite-based medium-resolution remote sensing makes possible the extraction of long time data series of consistent and comparable data. Furthermore, some satellite platforms offer free access to visible and multispectral data, such as Landsat 7–8. But these medium resolution satellites alone are insufficient for detecting and monitoring vegetation change caused by CO<sub>2</sub> leakage because the spatial resolution (e.g. 30 m for Landsat) and the orbit period (e.g. 16 days for Landsat) are inadequate (too coarse) for the purpose.

Accessing high or very high spatial resolution imagery (i.e. few meters or better) with daily (or better) revisiting times has only become possible recently through commercial satellites. The launch of successful small satellite missions, particularly nanosatellites, has resulted in the generation of larger observation constellations. They are able to achieve high temporal resolution of data and in the meantime possess very high spatial resolution. For example, with more than 170 satellites in orbit at present, the Planet constellation scans the Earth every day, imaging the entirety of Earth's landmass at 3–5 m resolution. Intensive monitoring of vegetation for specific area at high resolution is thus possible. However, this imagery is still expensive and not practical to use for large-area and long-time vegetation monitoring.

Airborne systems have the advantage over satellites that they

provide simple and reliable means of acquiring remotely sensed images. They can fly on demand, they are not limited by cloud cover as they can fly beneath it, and they are not constrained by an orbit and so can cover an area as often as is necessary. In addition, the remote sensing equipment carried may be able to give greater spectral resolution, for example the hyperspectral sensors which cover a range of 440–2500 nm with over 100 wavebands. Airborne hyperspectral imaging obtains imagery with adequate spatial resolution and improved spectral resolution capable of detecting leaks. This would probably be suitable for monitoring leakage if weather conditions allow images to be collected (ideally clear sky), although some argued it may be cost prohibitive due to the requirement of relatively expensive aircraft and pilot. The UAV platforms have become more widespread in recent years with affordable aircraft and camera payloads ranging from visible, near and thermal infrared, and 3D LIDAR. Using the UAV, higher spatial and temporal data resolution can be achieved, which makes possible vegetation detection to the sub-meter resolution.

Operational systems using medium-high resolution satellites have promise for large-area monitoring of environmental impact. Enormous data with different spatial, temporal and spectral resolutions from various sensors can be integrated and compensated in such systems. Large amounts of other geospatial data, such as land cover, land use, climate, hydrology and topography, can also be incorporated. With the advanced analysis capability of algorithms and models in the system, natural and human-induced vegetation changes can be clarified for providing management insights and decision support. The output will be definitely useful to the identification of the CO<sub>2</sub> leakage impact on vegetation. In addition, the system is usually implemented as an online tool which is simple to operate, easy to understand, and free to access. It would negate many of the costs of supporting large numbers of users for timelier data delivery.

Phenocams provide data at local and landscape scales that can be

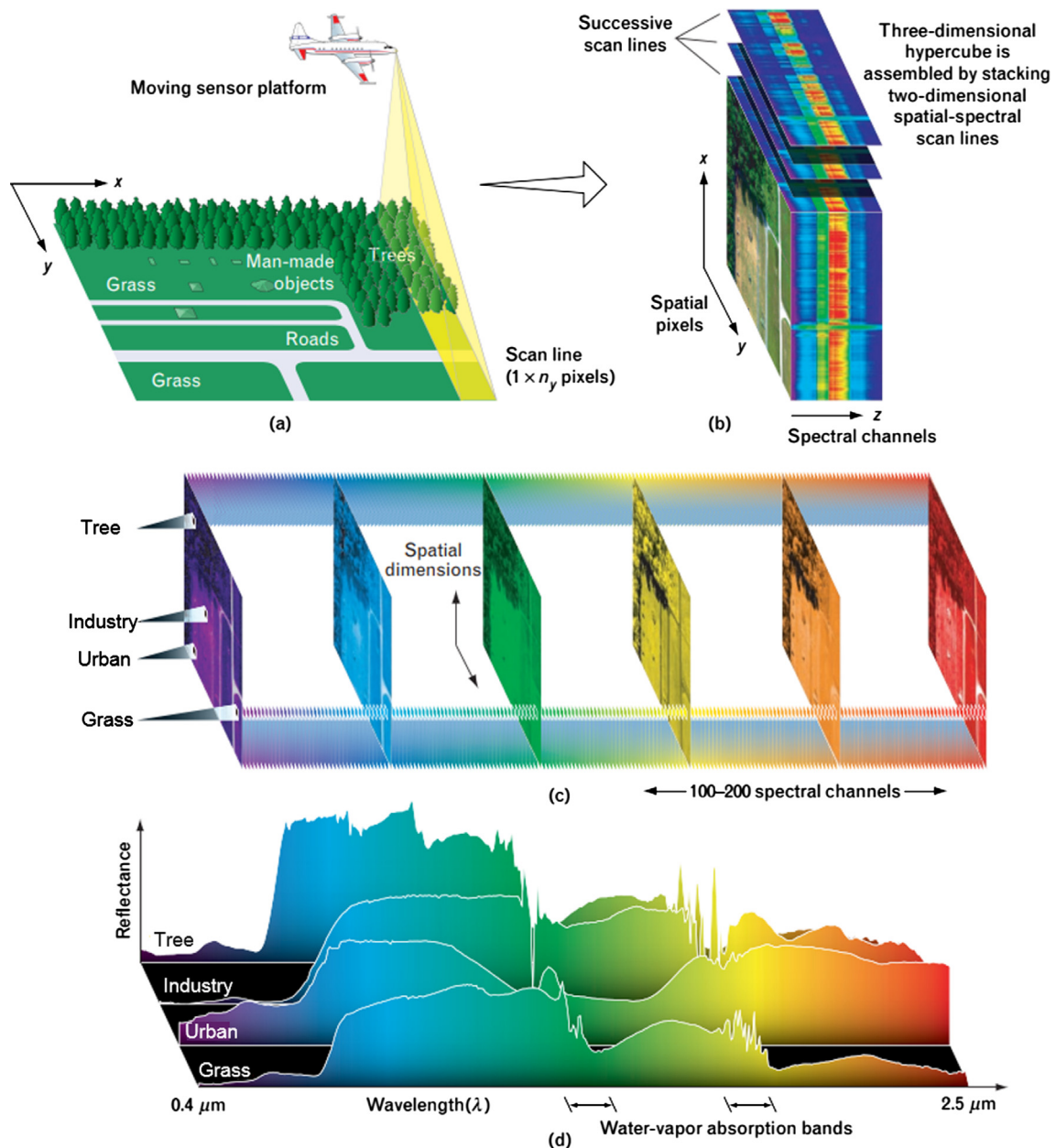


**Fig. 2.** Structure of the hyperspectral data cube. (a) A push-broom sensor on an airborne or spaceborne platform collects spectral information for a one-dimensional row of cross-track pixels, called a scan line. (b) Successive scan lines comprised of the spectra for each row of cross-track pixels are stacked to obtain a three-dimensional hyperspectral data cube. In this illustration the spatial information of a scene is represented by the x and y dimensions of the cube, while the amplitude spectra of the pixels are projected into the z dimension. (c) The assembled three-dimensional hyperspectral data cube can be treated as a stack of two-dimensional spatial images, each corresponding to a particular narrow waveband. A hyperspectral data cube typically consists of hundreds of such stacked images. (d) Alternately, the spectral samples can be plotted for each pixel or for each class of material in the hyperspectral image. Distinguishing features in the spectra provide the primary mechanism for detection and classification of materials in a scene (by permission, from Shaw and Burke [27], *Lincoln Laboratory Journal*, 14, 3–28).

**Table 5**  
A comparison of commonly used imaging spectrometers.

Sensor	Organisation <sup>1</sup>	Country	Bands	Wavelength (nm)	Resolution
HYMAP	HyVista Corporation	Australia	128	400–2450	< 5 m
AVIRIS	NASA	United States	224	400–2500	20 m
AISA	Spectral Imaging Limited	Finland	286	450–900	1 m
CASI	ITRES Research Limited	Canada	288	430–870	0.25–1.5 m
DAIS 2115	Ger CORP	United States	211	400–1200	10 nm
PROBE-1	Earth Search Sciences Inc	United States	128	400–2450	1 nm





Fig. 3. Multirotor-based remote sensing system over farmers' fields in Tanzania. Photo courtesy of Roberto Quiroz, International Potato Centre.

used in diverse ways. The “near-remote sensing” of vegetation and landscapes by phenocams has advantages over satellite-derived data including imagery that is continuous in time, unaffected by cloud cover and finer scale information at the canopy level down to individual plants. Phenocam images also provide *in situ* details on mechanisms of changes viewed by satellite, such as the relationship of leaf color to satellite reflectance data, and landscape context for field observations.

### 3. Remote sensing of vegetation stress

#### 3.1. Remote sensing of chlorophyll content/concentration

Vegetation health is one of the most important measures of environmental impact of CO<sub>2</sub> leakage. Vegetation will be stressed due to elevated soil CO<sub>2</sub> concentration leading to decreased soil pH and decreased soil O<sub>2</sub> concentrations. Chlorosis, (yellowing) of leaf tissue due to a lack of chlorophyll, is a common indicator of vegetation under stress [13,34].

Healthy vegetation has a characteristic spectral signature in the solar radiation wavebands (Fig. 5). It has low reflectance (typically about 5%) in the visible wavebands (400–700 nm) and a very steep rise at about 700 nm to about 50% reflectance in the near-infrared (NIR). This spectral signature can be explained by the structure and chemical composition of the leaf. Leaves contain chlorophyll and other pigments such as carotenes, xanthophylls, anthocyanin and amaranthine that absorb light strongly in the visible wavelengths, and therefore, have low reflectance.

Chlorophyll, the major absorber of light in leaves, is contained mainly in the palisade tissue layer and comprises two forms. Chlorophyll *a* is found in all, and chlorophyll *b* in most,

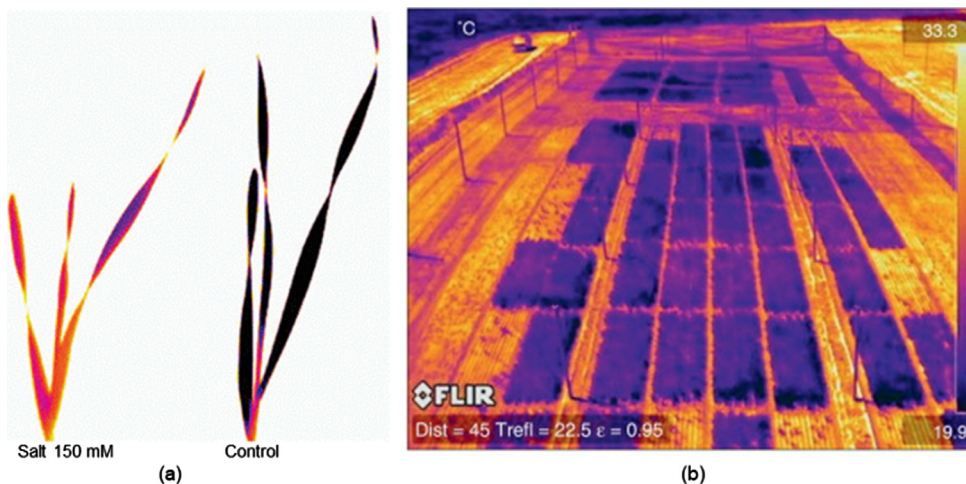


Fig. 4. Thermal images showing the difference in conditions with and without salt. (a) durum wheat seedlings to show leaf temperature difference ( $\sim 1^\circ\text{C}$ ) in a salt-stressed seedling relative to a control (non-salt seedling), and (b) a wheat trial imaged from a cherry picker to capture canopy temperature data for a large number of plots (by permission, from Furbank and Tester [33], *Trends in Plant Science*, 16, 635–44).

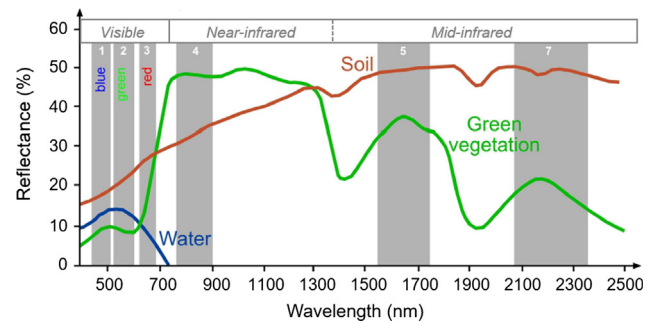


Fig. 5. Typical spectral signature of green vegetation, water and soil (modified from Siegmund and Menz [35]). Grey bands indicate Landsat wavelengths. (For interpretation of the references to color in this figure legend, the reader is referred to the web version of this article.)

photosynthesising plants. Changes in the level of chlorophyll in the leaf can be detected as changes in the spectral characteristics of the leaf, particularly in the visible wavelengths. Most other pigments absorb in the blue region in the vicinity of 445 nm, but only chlorophyll absorbs in the red at 645 nm [36]. Near-infrared light is not significantly absorbed or transmitted by pigments in the leaf and thus the reflectance is greater beyond 700 nm. At longer wavelengths (beyond 1350 nm) there is a decrease in reflectance as more radiation is absorbed by water within the leaf. The structure of the leaf, with many air–water interfaces, makes a very strong scattering medium that causes high reflectance and transmittance in any region where absorbance is low [37].

Chlorosis can be identified as a stress by remote sensing as an increase in reflectance in the yellow wavelengths at around 580 nm [37,38]. The sharp change in reflectance between wavelengths at around 690 and 740 nm is termed the “red-edge” [37,39]. It characterises the boundary between the strong absorption of red light by chlorophyll and the increased multiple scattering of radiation in the leaf mesophyll and the absence of absorption by pigments in the near-infrared wavelengths. Information on the red-edge position provides a useful indicator of chlorophyll content, which can then be used as an indicator of vegetation productivity or stress.

Many studies have been carried out to correlate spectral variations with chlorophyll content, and thus enable detection of stress by measuring decreased chlorophyll content. For example, Horler et al. [38] found that chlorotic leaves had higher reflectance in the visible wavelengths, with the effect greatest at 540 nm and that the red-edge was shifted towards shorter wavelengths. The chlorophyll content of a leaf was closely correlated with the red edge shift. Carter [40] used various stresses and plant species to detect changes in reflectance. He found

that visible reflectance, particularly in the region near 550 and 710 nm, increased consistently in response to stress regardless of the stress agent or the species. The greatest changes occurred near 710 nm. Close correlation between chlorophyll content and reflectance at 550 and 700 nm was also found by Gitelson and Merzylak [41], who found that reflectance near 700 nm and in the range 530–630 nm were the only features to be sensitive to chlorophyll content over a wide range of chlorophyll variation. Chappelle et al. [42] found that the concentration of chlorophyll *a* had a strong linear relationship with the reflectance ratio  $R_{675}/R_{700}$ , (where  $R_{675}$  is the reflectance at 675 nm and  $R_{700}$  is the reflectance at 700 nm), whereas the concentration of chlorophyll *b* was related best to  $R_{675}/(R_{675} \times R_{700})$ . Although this may work well at the leaf level it is not so consistent for canopies due to the effect of variations in background properties, and the effect of leaf layering and canopy structure. A pigment-specific simple ratio,  $PSSR = R_{800}/R_{680}$  was found by Blackburn [43] to have the strongest linear relationship with chlorophyll concentration in canopies. The optimum individual waveband for pigment estimation was 680 nm for chlorophyll *a*, 635 nm for chlorophyll *b* and 470 nm for carotenoids.

The stress can be induced by a variety of natural and anthropogenic stressors. Stress effects in plants may manifest themselves by showing decreased or increased growth (hyperplasia) or decreased levels of chlorophyll leading to chlorosis of the leaves and thus decreased photosynthesis. These changes could be detected using remote sensing. It should be possible to show that vegetation is stressed, but it is difficult to identify exactly what is causing the stress as plants tend to have a number of similar responses to a range of stresses. For example, although chlorosis can be detected, it is difficult to determine the cause of the response, because chlorosis is a general plant response to many stresses, such as drought, waterlogging, diseases and mineral deficiencies, as examples given in Table 6. One possible solution for this issue is to pay particular attention to the spatial arrangement of the anomalies as vegetation anomalies produced by  $CO_2$  leaks will have different sizes, shapes and patterns than those produced by water deficiency, grazing, machinery transit and so on [9]. Given the spatial feature (1–15 m) of possible leak impacts on vegetation [20–22], hyperspectral imaging could be a suitable means for the detection of leak-related vegetation stress.

### 3.2. $CO_2$ related stress detection using hyperspectral imaging

Hyperspectral remote sensing has been used in environmental monitoring, such as productivity evaluation, degradation assessment, carbon flux and storage estimate and response to disturbance or stress (human activities, grazing, fire and climate change). But there are limited studies on detection and monitoring  $CO_2$  leakage impact on ground cover. Among 19 relevant publications we found (Table 7) in the literature, the commonly used methods were mature techniques, such as linear regressions, time series analysis and vegetation indices (VIs).

Vegetation indices are simple and effective algorithms for

quantitative and qualitative assessment of vegetation cover condition among other approaches and applications [52]. Noomen et al. [53] examined the performance of 51 hyperspectral indices for detecting variations in canopy reflectance of maize and wheat caused by underground natural gas leakage. The effect of gas leakage on vegetation is similar to that of  $CO_2$ . When hydrocarbon seeps into the environment and into the roots of growing plants, it leads to stress as well as chlorosis. In the study, most indices that are known to respond to changes in vegetation vigour are reflectance ratios in the visible and near-infrared, while a few indices are located in the shortwave infrared. They found the indices had the highest correlation with oxygen concentrations in the soil for both species 29 days after a simulated gas leak, which was halfway through the growth cycle of the plants. It was not possible to find one reflectance index that could be used at any time during the growth cycle due to the changing canopy characteristics. Whereas Optimised Soil-Adjusted Vegetation Index (OSAVI) was the best predictor (at Day 29) based on the differences in canopy cover, Carter Indices (CTR2) was the best predictor (at Day 22) because of the less dense canopy and larger differences in leaf chlorophyll concentrations. Another study by Jiang et al. [54] showed the usefulness of the ratio of two sums, the first derivative reflectance in the green band ( $SD_g$ ) and red band ( $SD_r$ ). The index was suitable to identify  $CO_2$  leakage spots though monitoring the spectral change of vegetation on the surface of the CCS fields for both leaf scale and canopy scale. It was sensitive to bean under  $CO_2$  leakage stress and capable of distinguishing the gassed and ungassed bean in the slight  $CO_2$  leakage spots. The index could identify the bean stress on the 11th day after gassing started by utilizing leaf spectra, and it was also able to detect responses of bean by using canopy spectra after the twenty-second day since injection began. Therefore, their study suggested that it is possible to detect the  $CO_2$  leaking region by using hyperspectral remote sensing techniques.  $CO_2$  leakages may occur in the area where the index values fall significantly below the control values of the surrounding plants. Therefore, if abnormal index values were observed in some spots above sequestration fields, such spots could be considered as suspected leakage region.

### 3.3. Vegetation monitoring

#### 3.3.1. Assessment of baseline for impact

The overarching goal of a proposed monitoring plan is to assess status and trends of vegetation responses to  $CO_2$  leakage. A well-known sampling framework in ecology is the BACI (Before-After, Control-Impact) proposed by Stewart-Oaten et al. [69] to structure environmental impact monitoring. The BACI concept requires examination of the Before (pre-construction baseline) and After (post-construction) conditions of the area, as well as a comparison between a Reference site (without CCS) and the Impact site (with CCS). Before and After sampling will determine how the leakage process changed the site through time from its historical condition. Reference and Impact sampling will allow the effects of  $CO_2$  leakage to be discerned from natural variability, stochastic events, and underlying trends in the larger area.

**Table 6**

Remote sensing of vegetation stress-vegetation response to different stressor at identified wavelengths.

Wavelength (nm)	Stressor	Vegetation response	References
525–575	Nutrient deficiency	Increase in reflectance and shift to shorter wavelengths of the red-edge	[44]
550–650	Nutrient deficiency	Increase in reflectance and shift to shorter wavelengths of the red-edge	[45]
550 and 770	Waterlogging	Elevated reflectance	[46]
555 and 700	Nutrient deficiency	Greatest variations in reflectance	[47]
580	Drought	Increase in reflectance	[37]
650–850	Waterlogging	A small peak of reflectance	[48]
675	Drought	Increase in reflectance and shift to shorter wavelengths of the red-edge	[38]
690–700 and	Drought	High reflectance	[4950]
$R_{694}/R_{760}$		Increase in reflectance	
584 and 1300	Drought	Peak value of reflectance	[40]
1300–2500	Drought	Greatest increase in reflectance	[51]

**Table 7**

Summary of vegetation being detected/monitored (target), wavelength region studied and algorithm/model employed in literature on hyperspectral imaging of CO<sub>2</sub> leakage on rangelands.

Target	Wavelength (nm)	Algorithm/Model	Reference
Buffel grass	645–696, 765–815	Normalized Difference Vegetation Index (NDVI)	[25]
	2000, 2100, 2200	Cellulose Absorption Index (CAI)	
	705–750	Red Edge NDVI (RENDVI)	
	720–740	Vogelmann Red Edge Index 1 (VREI1)	
	1510, 1680	Normalised Difference Nitrogen Index (NDNI)	
	550, 680, 750	Plant Senescence Reflectance Index (PSRI)	
	510, 550, 700	Column Labels Carotenoid Reflectance Index (CLCRI)	
Bean	500–550, 680–760	Ratio of the sum of the first derivative reflectance in green band (SD <sub>g</sub> ) and red band (SD <sub>r</sub> ): SD <sub>r</sub> /SD <sub>g</sub>	[54]
Barley, canola and field pea	400–1000, 990–2494	Chlorophyll Normalized Difference Index (Chl NDI)	[2255]
Alfalfa	1300–2500	TIBCO Spotfire S+	
Alfalfa, dandelion, thistle	424–929	Red Edge Index (REI)	[56]
Western salsify, dandelion, Canada thistle, alfalfa, birdsfoot, trefoil, clover, lupine, quack grass, orchard grass, Kentucky bluegrass	630–670, 780–820	NDVI	[57]
Buffel grass	1360–1430, 1800–1950	NDVI	[58]
Grassland	402–989	Spectral mixture analysis (SMA)	[59]
		Intrinsic Random Functions (IRF)	
Vegetation	402–989	Generalised covariance function (GCF)	[60]
Western salsify, dandelion, Canada thistle, alfalfa, birdsfoot, trefoil, clover, lupine, quack grass, orchard grass, Kentucky bluegrass	700–760	Point Spread Function (PSF)	
Tall and underlying grasses	500–580, 630–710, 735–865	Linear Regressions	[61]
Flower, Orchard grass, Kentucky bluegrass	575–580, 720–723	NDVI	[62]
		Structural Independent Pigment Index (SIPI)	
		Normalized Difference First Derivative Index (NFDI)	
		Chl NDI	
Vegetation	350–2500	Pigment Specific Simple Ratios (both PSSRa and PSSRb)	[64]
Alfalfa	650–750	Analysis of Time Series (ATS)	
40–50 cm grass (May), < 15 cm grass (Oct)	402–989	Random Forest Classifiers (RFC)	[65]
Maize, wheat	350–2500	Normal Probability Plot (NPP)	[66]
Maize, wheat, grassland	400–2170	Optimised Soil-Adjusted Vegetation Index (OSAVI)	[53]
		Carter Indices (CTR2) and 49 others	
Grass, wheat, bean	702, 720–730	Lichtenthaler Indices (LIC)	[67]
Soybean	410–740	Derivative Analysis (DA)	[68]
		Regamma Function (RF)	[49]

A Reference site which has identical conditions to the Impact site is usually unavailable. Thus, areas near the CCS but not part of the area directly affected by the injection can be used as Reference sites. The Impact and Reference sites are typically monitored with similar intensity to allow for direct comparison of the different monitoring samples.

### 3.3.2. Integration of multi-sensors and multi-data

With the advances in sensor technology and the increasing quantity of multi-sensor, multi-temporal, and multi-resolution data from different sources over the last decade, data integration has become a valuable approach in detecting and monitoring the effect of CO<sub>2</sub> leakage on vegetation. It aims synergistically combine sensor data from disparate sources – with different characteristics, resolution, and quality – in order to provide more reliable, accurate, and useful information required for the application purpose. Olsson et al. [58] used both hyperspectral field measurements and Landsat TM imagery to detect invasive grass in a desert scrub community in USA. They integrated field measurements of hyperspectral plant species signatures and canopy cover with multi-temporal spectral analysis to identify opportunities for detection using moderate-resolution multi-spectral imagery. They found Landsat TM-based reflectance differences of uninvaded and invaded landscapes are minimal due to the high level of mixing, and a sensor with narrow bands at 2050, 2100, and 2150 nm would be essential for the detection. Marshall et al. [70] conducted a study to determine if Worldview-2 8-band multispectral imagery can be used to discriminate grass in Australia. Their results proved Worldview-2 offers even greater potential for the discrimination of buffel grass under NIR2 (near-infrared 2: 860–1040 nm) and Yellow

(608–632 nm) bands. Marshall et al. [30] undertook another study aiming at assessing the feasibility of using airborne imagery for vegetation assessment in Australian arid lands. They evaluated the common methods using high-resolution multispectral imagery and aerial photography, and recommended that an ultra-high resolution aerial photography together with airborne hyperspectral imagery could be considered for improved spectral separation. Sandino et al. [71] proposed an integrated pipeline methodology for monitoring vegetation in arid and semiarid Australia. They demonstrated the implementation of unmanned aerial systems (UAVs and high-resolution RGB cameras) and machine learning for a feasible, accurate and light-weighted assessment of grasses (buffel and spinifex). Most recently, Guerschman et al. [25] investigated a suite of related VIs at a proposed Australian CCS site where vegetation cover is highly variable in spatial and temporal dimensions following environmental and human-induced drivers. They conducted a baseline assessment of vegetation condition on rangelands dominated by buffel grass using Landsat and HyMap hyperspectral imagery in combination with a field survey. The analysis of time series of satellite data (Landsat-derived vegetation fractional cover) spanning 30 years show how vegetation changes within season and the specific trends of each part of study site since 1988 (Fig. 6). They were also able to identify areas cropped in the past and disturbed by some other type of land uses. Their study proved that hyperspectral imagery provides a much more spatially detailed picture of the vegetation condition at just one moment in time. It also proves its ability to accurately map (Fig. 7) and identify specific traits of vegetation condition (particularly cover and green/non-green fractions) at the image resolution (1.8 m).

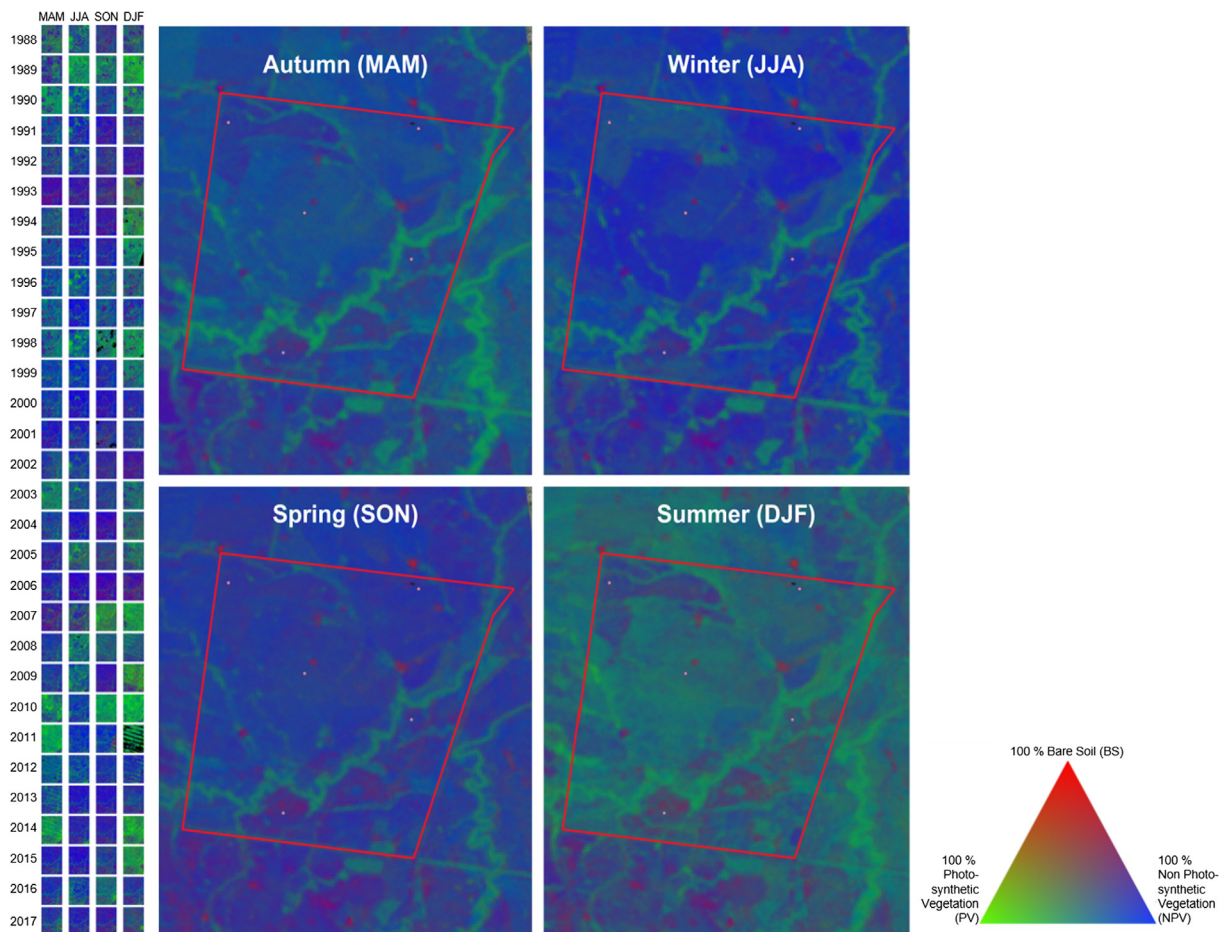


**Fig. 6.** Maps showing the fractional cover (1988–2017) at a planned CCS area. The left panel shows all Landsat images for four seasons from 1988 to 2017. The four larger maps show the long-term mean cover for Autumn (Mar–Apr–May, or MAM), Winter (Jun–Jul–Aug, or JJA), Spring (Sep–Oct–Nov, or SON) and Summer (Dec–Jan–Feb, or DJF). Yellow dots represent five study sites. (For interpretation of the references to color in this figure legend, the reader is referred to the web version of this article.)

### 3.4. Discussion

Achieving both high spatial resolution and high spectral resolution is an important direction of the most recent advances in remote sensing technology for vegetation stress detection. Hyperspectral imaging meets the needs of enabling small leakage features, or vegetation responses to leakage, to be successfully captured. Although there has been a significant increase in scientific literature in recent years focusing on detecting stress in plants using hyperspectral image analysis, applications of hyperspectral imaging in monitoring the impact of CO<sub>2</sub> on vegetation are limited. The technology is becoming more popular since the falling costs of camera production have enabled researchers and developers greater access to this technology. But it still has two major issues. One is its small scene coverage, making them unsuitable for mapping large areas. The other is its revisit frequency, which makes the CO<sub>2</sub> leakage monitoring difficult.

There are various techniques available to analyse the data to detect CO<sub>2</sub> induced stress in plants. Examples of these methods have been discussed in this section. Vegetation and stress indices are increasing in quantity every year. Significant wavelengths combined together can indicate the health status occurring within a specific species. Indices are valuable for detecting specific criteria for vegetation only when they are selected with the datasets, species and conditions favourable to the experiments at that time. It is difficult to take an index designed for plant X and apply it to a dataset for plant Y. This is the motivation behind considering a larger range of wavelengths over the spectrum, which has the potential to yield better results.

It is relatively easy to detect vegetation stresses, but much more difficult to identify those caused by CO<sub>2</sub> leaks from others, such as natural climate variability, grazing and other human interventions. One possible solution for this issue is to pay particular attention to the spatial pattern of the stress as vegetation stress produced by CO<sub>2</sub> leaks will have a different size and shape than that produced by water deficiency, grazing, harvesting and so on [9]. Another effective way is to conduct a baseline assessment of ‘intact’ condition before injection and undertake evaluation in comparison with a reference site after injection.

A hyperspectral image acquisition can be a good option for assessing vegetation condition if a leak is detected and/or at regular intervals after the commencement of the CO<sub>2</sub> injection. However, the cost is relatively high. Cheaper options (and faster and more flexible to deploy) can be sourced from UAV providers. The exact characteristics of the imagery being acquired need to be carefully assessed, particularly in the context of an increasing number of providers and specifications available. At the very least, a multispectral sensor can be used to capture the red edge features. In addition to the above, phenocams are a cheap and reliable source of *in situ* information and can track daily changes in vegetation and therefore be a rapid way to detect sudden changes in vegetation conditions.

Vegetation monitoring on its own is not going to provide a reliable way of detecting CO<sub>2</sub> leakage. Rather, it has to be a complement of other more direct tracking of CO<sub>2</sub> levels on the ground and in the atmosphere. The main reason is that the stresses in vegetation induced by CO<sub>2</sub> in the soil produce similar effects to other stresses such as water or

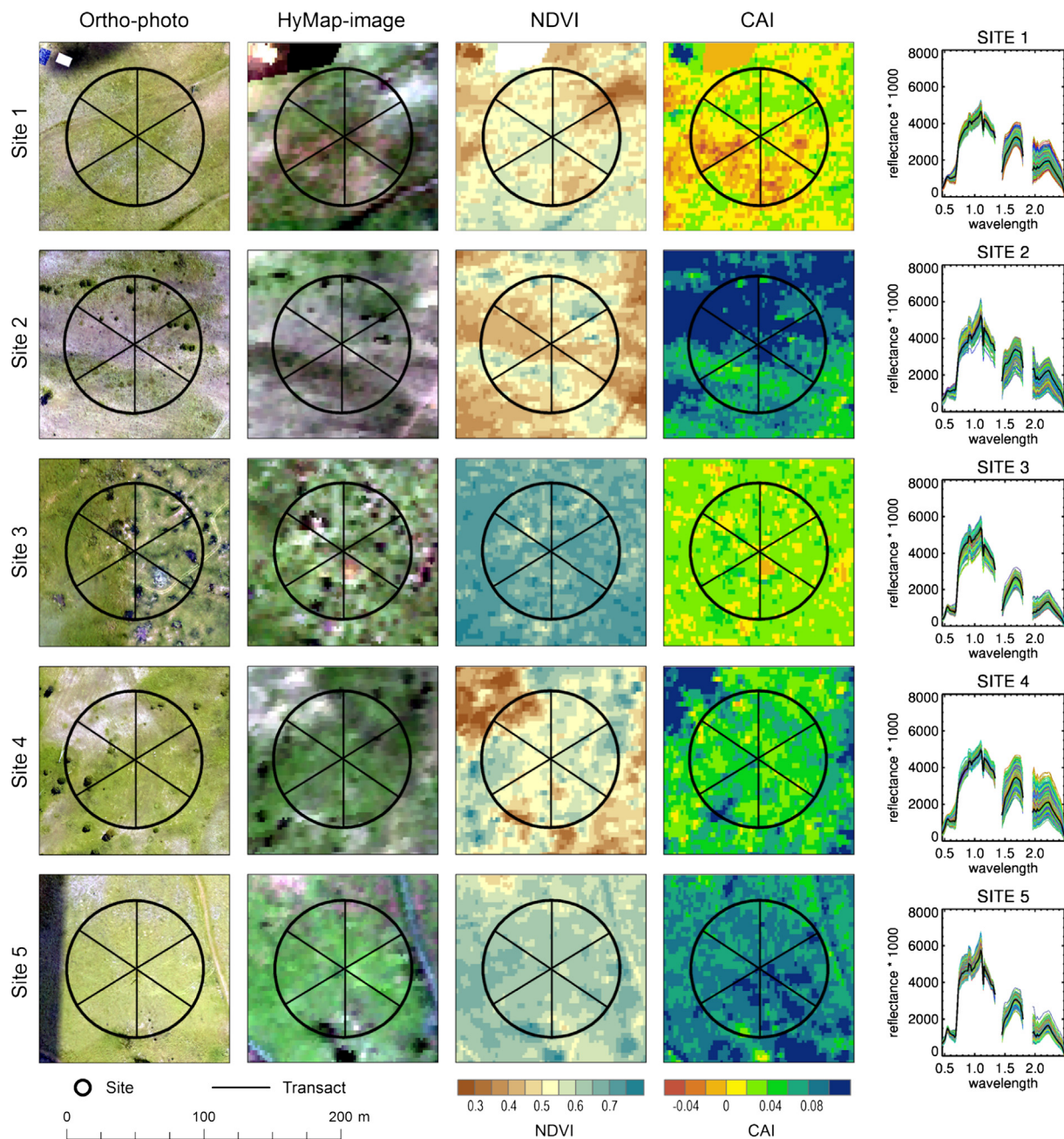


Fig. 7. Orthophotos (15 cm resolution; 1st column from left), HyMap in false color (1.8 m resolution; 2nd column from left) and vegetation indices (3rd and 4th columns from left) derived from the HyMap image for the five study sites in Fig. 6. Spectra for all pixels (in color) and mean spectra for each site (black line) are shown in the right-hand side column. NDVI stands for Normalised Difference Nitrogen Index, and CAI is Cellulose Absorption Index. (For interpretation of the references to color in this figure legend, the reader is referred to the web version of this article.)

nutrient deficiency, and therefore the rates of false positives would be too high and difficult to reduce.

#### 4. Recommendations for establishing a monitoring system

##### 4.1. Remote sensing is a feasible means for vegetation monitoring

CCS is an emerging climate change mitigation technology and environmental monitoring is vital for its credibility as a sustainable solution. Satellite, airborne and in-situ remote sensing provides a cost-effective technique for monitoring vegetation condition and potentially identifies CO<sub>2</sub> leakage through the detection of plant stress caused by elevated soil CO<sub>2</sub> associated with CCS sites.

##### 4.2. Combination of several remotely-sensed sources and on-ground monitoring is the most promising alternative

The particular characteristics of the effects of CO<sub>2</sub> leaks on vegetation (small hot spots producing plant chlorosis) determine that no single approach can, on its own, be sufficient for continuous monitoring of an operational CCS facility.

We recommend that a system is put in place combining the following technologies:

- Continuous monitoring using medium resolution (Landsat, Sentinel 2) satellite remote sensing sources: This option is cheap (data sources are free), can monitor a large area and can compare any given point in time with the condition in the same location in the

past. These data sources, however, do not have sufficient spatial resolution for identifying small hot spots of plant stress in case of CO<sub>2</sub> leaks occurrence. Tools such as the VegMachine described in Section 2.1.3 can be a useful technique already available for this.

- *Ad-hoc* acquisition of high-resolution aerial imagery (ideally hyperspectral) following specific detected CO<sub>2</sub> leaking events: In the hypothetical case that a CO<sub>2</sub> leak is registered, a high-resolution hyperspectral image of the affected area can assist in pinpointing the spatial extent of stress caused to vegetation.
- Continuous monitoring of the injection point(s) using phenocams: as the leaks, if they occur, are more likely to occur near the injection points, we recommend continuous monitoring of these areas using hyperspectral phenocams installed on site.

#### 4.3. Reference site selection and baseline assessment are essential for CO<sub>2</sub> leakage detection

It is important to understand whether different sources of physiological plant stress occur naturally and are spectrally discernible in order to properly interpret vegetation stress signals during image analysis. It is expected that the highly dimensional nature of hyperspectral data lends itself to discriminate among different types of vegetation stress. However, our literature search shows even though hyperspectral signatures can be used to estimate the amount of plant stress, it is unable to distinguish between the different causes of stress. This uncertainty can be problematic when testing for CO<sub>2</sub> leaks. A CCS field could appear unhealthy spectrally, but the stress could be caused by other plant physiological stressors. To reduce the number of possible false positives, it is important to normalise measurements by comparing plant spectra to identical environmental conditions outside the site. In this case, the selection of reference sites become significantly important. Similarly, to distinguish between the concepts of “environmental impact” and “leakage effect”, acquiring baseline characterization of environmentally-relevant variables is crucial to this distinction.

We then recommend that:

- An aerial hyperspectral image is acquired in a CCS planned site before any CO<sub>2</sub> injection begins and the naturally occurring variability in vegetation condition is assessed, particularly those traits known to be affected by CO<sub>2</sub> leaks.
- An assessment of the natural and human-induced variability in vegetation cover in the planned injection site is performed using long-term data obtained from the Landsat sensor. This assessment will determine the range of conditions observed in each 30 × 30 m pixel over the last 27 years and can be used as a baseline for tracking any future anomalies in vegetation cover.

In conclusion, a primary concern for the safety and effectiveness of CCS is the possibility that CO<sub>2</sub> may migrate from storage sites to the Earth's surface. Direct detection of CO<sub>2</sub> leaks via its effects on vegetation are highly difficult due to the small nature of the area affected and the high chances of false positives. Our review has addressed this challenge. It adds value to the literature by recommending an integrated monitoring system where remote sensing technology is a key driver. The recommended approach provides scientific rigour to meet public expectations of the sustainability of the CCS practice for bridging the gaps between research, development and implementation of CCS. It is crucial to the minimisation of environmental impacts for a sustainable CCS implementation, and will eventually contribute to environmental pollution reduction and climate change mitigation.

#### Acknowledgements

This study contributes to the Remote Sensing of Vegetation Condition Monitoring project supported by the Australian National Low Emissions Coal Research and Development (ANLEC R&D). We thank

our colleagues Dr. Philip Ford and Susan Cuddy for reviewing and editing the manuscript.

#### References

- [1] IPCC. Climate change 2014: mitigation of climate change. In: Edenhofer O, Pichs-Madruga R, Sokona Y, Farahani E, Kadner S, Seyboth K, editors. Contribution of working group III to the fifth assessment report of the intergovernmental panel on climate change. Cambridge, UK and New York, NY, USA: Cambridge University Press; 2014.
- [2] IPCC (Intergovernmental Panel on Climate Change). IPCC Special Report on Carbon Dioxide Capture and Storage: Prepared by Working Group III of the Intergovernmental Panel on Climate Change. In: Metz B, Davidson O, De Coninck HC, Loos M, Meyer LA, editors. Cambridge, UK and New York, NY, USA: Cambridge University Press; 2005. p. 442.
- [3] Benson S, Cook P. Underground geological storage. In: Metz B, Davidson O, de Coninck H, Loos M, Meyer L, editors. IPCC special report on carbon dioxide capture and storage. Cambridge, England: Cambridge University Press; 2005.
- [4] Hepple RP, Benson SM. Geologic storage of carbon dioxide as a climate change mitigation strategy: performance requirements and the implications of surface seepage. *Environ Geol* 2005;47:576–85.
- [5] Deng H, Bielicki JM, Oppenheimer M, Fitts JP, Peters CA. Leakage risks of geologic CO<sub>2</sub> storage and the impacts on the global energy system and climate change mitigation. *Clim Change* 2017;144:151–63.
- [6] Pierce S, Sjögersten S. Effects of below ground CO<sub>2</sub> emissions on plant and microbial communities. *Plant Soil* 2009;325:197.
- [7] Plasynski SI, Litynski JT, McIlvried HG, Vikara DM, Srivastava RD. The critical role of monitoring, verification, and accounting for geologic carbon dioxide storage projects. *Environ Geosci* 2011;18:19–34.
- [8] Verkerke JL, Williams DJ, Thoma E. Remote sensing of CO<sub>2</sub> leakage from geologic sequestration projects. *Int J Appl Earth Obs* 2014;31:67–77.
- [9] Feitz A, Leamon G, Jenkins C, Jones DG, Moreira A, Bressan L, et al. Looking for leakage or monitoring for public assurance? *Energy Procedia* 2014;63:3881–90.
- [10] Lewicki JL, Oldenburg CM, Dobeck L, Spangler L. CO<sub>2</sub> leakage during two shallow subsurface CO<sub>2</sub> releases. *Geophys Res Lett* 2007;34:L24402.
- [11] Humphries SD, Nehrir AR, Keith CJ, Repasky KS, Dobeck L, Carlsten L, et al. Testing carbon sequestration site monitoring instruments using a controlled carbon dioxide release facility. *Appl Opt* 2008;47:548–55.
- [12] Lewicki JL, Hilley GE. Eddy covariance mapping and quantification of surface CO<sub>2</sub> leakage fluxes. *Geophys Res Lett* 2009;36:L21802.
- [13] Krüger M, Jones D, Frerichs J, Oppermann BI, West J, Coombs P, et al. Effects of elevated CO<sub>2</sub> concentrations on the vegetation and microbial populations at a terrestrial CO<sub>2</sub> vent at Laacher See, Germany. *Int J Greenh Gas Con* 2011;5:1093–8.
- [14] Jenkins C, Chadwick A, Hovorka SD. The state of the art in monitoring and verification-ten years on. *Int J Greenh Gas Con* 2015;40:312–49.
- [15] Amonette JE, Barr JL, Dobeck LM, Gullickson K, Walsh SJ. Spatiotemporal changes in CO<sub>2</sub> emissions during the second ZERT injection, August–September 2008. *Environ Earth Sci* 2010;60:263–72.
- [16] Al-Traboulsi M, Sjögersten S, Colls J, Steven M, Black C. Potential impact of CO<sub>2</sub> leakage from Carbon Capture and Storage (CCS) systems on growth and yield in maize. *Plant Soil* 2013;365:267–81.
- [17] Spangler LH, Dobeck LM, Repasky K. A controlled field pilot in Bozeman, Montana, USA, for testing near surface CO<sub>2</sub> detection techniques and transport models. *Environ Earth Sci* 2009;60:285–97.
- [18] Spangler LH, Dobeck LM, Repasky K, Nehrir A, Humphries S, Barr J, et al. A controlled field pilot for testing near surface CO<sub>2</sub> detection techniques and transport models. *Energy Procedia* 2009;1:2143–50.
- [19] Ko D, Yoo G, Yun ST, Chung H. Impacts of CO<sub>2</sub> leakage on plants and microorganisms: a review of results from CO<sub>2</sub> release experiments and storage sites. *Greenh Gases* 2016;6:319–38.
- [20] Smith KL. Remote sensing of leaf responses to leaking underground natural gas [PhD thesis]. UK: University of Nottingham; 2002.
- [21] Hoeks J. Changes in composition of soil air near leaks in natural gas mains. *Soil Sci* 1972;113:46–54.
- [22] Feitz A, Jenkins C, Schacht U, McGrath A, Berko H, Schroder I, et al. An assessment of near surface CO<sub>2</sub> leakage detection techniques under Australian conditions. *Energy Procedia* 2014;63:3891–906.
- [23] Chen Y, Guerschman J. Remote sensing for vegetation monitoring in Carbon Capture and Geological Storage projects: a review. Report to the Australian National Low Emissions Coal Research & Development (ANLEC) for the Vegetation Condition Monitoring (7-1116-0299) project; 2018.
- [24] Beutel T, Karfs R, Wallace J, Scarth P, Trevithick R, Tindall D. VegMachine® in Queensland. In: Friedel MH, editor. Innovation in the Rangelands. Proceedings of the 18th Australian rangeland society biennial conference, Alice Springs. Parkside, SA: Australian Rangeland Society; 2015.
- [25] Guerschman J, Chen Y, Cheng Z, Koopman S, Guo L. Baseline assessment of vegetation condition in Glenhaven Station. Final report to the Australian National Low Emissions Coal Research & Development (ANLEC) for the Vegetation Condition Monitoring (7-1116-0299) project; 2018.
- [26] Manolakis D, Lockwood R, Cooley T. Hyperspectral imaging remote sensing: physics, sensors, and algorithms. Cambridge University Press; 2016.
- [27] Shaw GA, Burke HK. Spectral imaging for remote sensing. *Linc Lab J* 2003;14:3–28.
- [28] Picon A, Ghita O, Whelan PF, Iriondo P. Fuzzy spectral and spatial feature integration for classification of non-ferrous materials in hyper-spectral data. *IEEE T*

- Ind Inform 2009;5:483–94.
- [29] Ran L, Zhang Y, Wei W, Zhang Q. A hyperspectral image classification framework with spatial pixel pair features. *Sensors* 2017;17:2421.
- [30] Marshall VM, Lewis MM, Ostendorf B. Detecting new Buffel grass infestations in Australian arid lands: evaluation of methods using high-resolution multispectral imagery and aerial photography. *Environ Monit Assess* 2014;186:1689–703.
- [31] Brown TB, Hultine KR, Steltzer H, Denny EG, Denslow MW, Granados J, et al. Using phenocams to monitor our changing Earth: toward a global phenocam network. *Front Ecol Environ* 2016;14:84–93.
- [32] Araus JL, Cairns JE. Field high-throughput phenotyping: the new crop breeding frontier. *Trends Plant Sci* 2014;19:52–61.
- [33] Furbank RT, Tester M. Phenomics-technologies to relieve the phenotyping bottleneck. *Trends Plant Sci* 2011;16:635–44.
- [34] Zhang X, Ma X, Zhao Z, Wu Y, Li Y. CO<sub>2</sub> leakage-induced vegetation decline is primarily driven by decreased soil O<sub>2</sub>. *J Environ Manage* 2016;171:225–30.
- [35] Siegmund A, Menz G. Fernes nah gebracht—Satelliten-und Luftbildeinsatz zur Analyse von Umweltveränderungen im Geographieunterricht. *Geogr Sch* 2005;154:2–10.
- [36] Gates DM, Keegan HJ, Schelter JC, Weidner VR. Spectral properties of plants. *Appl Opt* 1965;4:11–20.
- [37] Wooley JT. Reflectance and transmittance of light by leaves. *Plant Physiol* 1971;47:656–62.
- [38] Horler DN, Dockray M, Barber J. The red-edge of plant leaf reflectance. *Int J Remote Sens* 1983;4:273–88.
- [39] Curran PJ, Dungan JL, Macler BA, Plummer SE. The effect of red leaf pigment on the relationship between red-edge and chlorophyll concentration. *Remote Sens Environ* 1991;35:69–76.
- [40] Carter GA. Responses of leaf spectral reflectance to plant stress. *Am J Bot* 1993;80:239–43.
- [41] Gitelson A, Merzlyak MN. Remote estimation of chlorophyll content in higher plant leaves. *Int J Remote Sens* 1997;18:291–8.
- [42] Chappelle EW, Kim MS, McMurtrey III JE. Ratio analysis of reflectance spectra (RARS): an algorithm for the remote estimation of the concentrations of chlorophyll a, chlorophyll b, and carotenoids in soybean leaves. *Remote Sens Environ* 1992;39:239–47.
- [43] Blackburn GA. Quantifying chlorophylls and carotenoids at leaf and canopy scales: an evaluation of some hyperspectral approaches. *Remote Sens Environ* 1998;66:273–85.
- [44] Milton NM, Eisworth BA, Ager CM. Effect of phosphorus deficiency on spectral reflectance and morphology of soybean plants. *Remote Sens Environ* 1991;36:121–7.
- [45] Milton NM, Ager CM, Eisworth BA, Power MS. Arsenic-and selenium-induced changes in spectral reflectance and morphology of soybean plants. *Remote Sens Environ* 1989;30:263–9.
- [46] Anderson JE, Perry JE. Characterisation of wetland plant stress using leaf spectral reflectance: implications for wetland remote sensing. *Wetlands* 1996;16:477–87.
- [47] Masoni A, Ercoli L, Mariotti M. Spectral properties of leaves deficient in Iron, Sulphur, Magnesium and Manganese. *Agron J* 1996;88:937–43.
- [48] Pickerill JM, Malthus TJ. Leak detection from rural aqueducts using airborne remote sensing techniques. *Int J Remote Sens* 1998;19:2427–33.
- [49] Carter GA, Miller RL. Early detection of plant stress by digital imaging within narrow stress-sensitive wavebands. *Remote Sens Environ* 1994;50:295–302.
- [50] Carter GA, Cibula WG, Miller RL. Narrow band reflectance imagery compared with thermal imagery for early detection of plant stress. *J Plant Physiol* 1996;148:515–22.
- [51] Carter GA. Primary and secondary effects of water content on the spectral reflectance of leaves. *Am J Bot* 1991;91:6–24.
- [52] Chen Y, Gillieson D. Evaluation of Landsat TM vegetation indices for estimating vegetation cover on semi-arid rangelands: a case study from Australia. *Can J Remote Sens* 2009;35:435–46.
- [53] Noomen MF, Smith KL, Colls JJ, Steven MD, Skidmore AK, Van Der Meer FD. Hyperspectral indices for detecting changes in canopy reflectance as a result of underground natural gas leakage. *Int J Remote Sens* 2008;29:5987–6008.
- [54] Jiang JB, Steven MD, Cai QK, He RY, Guo HQ, Chen Y. Detecting bean stress response to CO<sub>2</sub> leakage with the utilization of leaf and canopy spectral derivative ratio. *Greenh Gases* 2014;4:468–80.
- [55] Bellante GJ, Powell SL, Lawrence RL, Repasky KS, Dougher T. Hyperspectral detection of a subsurface CO<sub>2</sub> Leak in the presence of water stressed vegetation. *PLoS ONE* 2014;9:e108299.
- [56] Bellante GJ, Powell SL, Lawrence RL, Repasky KS, Dougher TA. Aerial detection of a simulated CO<sub>2</sub> leak from a geologic sequestration site using hyperspectral imagery. *Int J Greenh Gas Con* 2013;13:124–37.
- [57] Hogan JA, Shaw JA, Lawrence RL, Lewicki JL, Dobeck LM, Spangler LH. Detection of leaking CO<sub>2</sub> gas with vegetation reflectance measured by a low-cost multispectral imager. *IEEE J Sel Top Appl Earth Obs Remote Sens* 2012;5:699–706.
- [58] Olsson AD, van Leeuwen WJ, Marsh SE. Feasibility of invasive grass detection in a deserts scrub community using hyperspectral field measurements and Landsat TM imagery. *Remote Sens* 2011;3:2283–304.
- [59] Govindan R, Korre A, Durucan S, Imrie CE. A geostatistical and probabilistic spectral image processing methodology for monitoring potential CO<sub>2</sub> leakages on the surface. *Int J Greenh Gas Con* 2011;5:589–97.
- [60] Govindan R, Korre A, Durucan S, Imrie CE. Comparative assessment of the performance of airborne and spaceborne spectral data for monitoring surface CO<sub>2</sub> leakages. *Energy Procedia* 2011;4:3421–7.
- [61] Hogan JA. Multi-spectral imaging of vegetation for CO<sub>2</sub> leak detection [Doctoral dissertation]. Montana State University-Bozeman, College of Engineering; 2011.
- [62] Rouse JH, Shaw JA, Lawrence RL, Lewicki JL, Dobeck LM, Repasky KS, et al. Multi-spectral imaging of vegetation for detecting CO<sub>2</sub> leaking from underground. *Environ Earth Sci* 2010;60:313–23.
- [63] Lakkaraju VR, Zhou X, Apple ME, Cunningham A, Dobeck LM, Gullickson K, et al. Studying the vegetation response to simulated leakage of sequestered CO<sub>2</sub> using spectral vegetation indices. *Ecol Inform* 2010;5:379–89.
- [64] Male EJ, Pickles WL, Silver EA, Hoffmann GD, Lewicki J, Apple M, et al. Using hyperspectral plant signatures for CO<sub>2</sub> leak detection during the 2008 ZERT CO<sub>2</sub> sequestration field experiment in Bozeman, Montana. *Environ Earth Sci* 2010;60:251–61.
- [65] Keith CJ, Repasky KS, Lawrence RL, Jay SC, Carlsten JL. Monitoring effects of a controlled subsurface carbon dioxide release on vegetation using a hyperspectral imager. *Int J Greenh Gas Con* 2009;3:626–32.
- [66] Bateson L, Vellico M, Beaubien SE, Pearce JM, Annunziatellis A, Ciotoli G, et al. The application of remote-sensing techniques to monitor CO<sub>2</sub>-storage sites for surface leakage: method development and testing at Latera (Italy) where naturally produced CO<sub>2</sub> is leaking to the atmosphere. *Int J Greenh Gas Con* 2008;2:388–400.
- [67] Noomen MF. Hyperspectral reflectance of vegetation affected by underground hydrocarbon gas seepage. Enschede, the Netherlands (ITC): International Institute for Geo-information Science & Earth Observation; 2007.
- [68] Smith KL, Steven MD, Colls JJ. Use of hyperspectral derivative ratios in the red-edge region to identify plant stress responses to gas leaks. *Remote Sens Environ* 2004;92:207–17.
- [69] Stewart-Oaten A, Murdoch WW, Parker KR. Environmental impact assessment: “Pseudoreplication” in time? *Ecology* 1986;67:929–40.
- [70] Marshall VM, Lewis MM, Ostendorf B. Do additional bands (coastal, NIR-2, red-edge and yellow) in WORLDVIEW-2 multispectral imagery improve discrimination of an invasive tussock, buffel grass (*Cenchrus ciliaris*)? In: International archives of the photogrammetry, remote sensing and spatial information sciences, XXII ISPRS Congress, Melbourne, Australia, XXXIX-B8; 2012. p. 277–81.
- [71] Sandino J, Gonzalez F, Mengersen K, Gaston KJ. UAVs and machine learning revolutionising invasive grass and vegetation surveys in remote arid lands. *Sensors* 2018;18:605.